A 10 km-resolution synthetic Venus gravity field model based on topography

Fei Li [a], Jianguo Yan [a,b,*], Luyuan Xu [c], Shuanggen Jin [d], J. Alexis P. Rodriguez [e], James H. Dohm [f]

[a] State Key Laboratory of Information Engineering in Surveying, Mapping and Remote Sensing, Wuhan University, Wuhan 430070, China
[b] RISE Project, National Astronomical Observatory of Japan, Oshu 0230861, Japan
[c] Chinese Antarctic Center of Surveying and Mapping, Wuhan University, Wuhan 430070, China
[d] Shanghai Astronomical Observatory, Chinese Academy of Sciences, Shanghai 20030, China
[e] NASA Ames Research Center, Mail Stop 239-20, Moffett Field, CA 94035, USA
[f] The University Museum, The University of Tokyo, Tokyo 1130033, Japan

ABSTRACT

A high resolution gravity field model is extremely important in the exploration of Venus. In this paper, we present a 3-dimensional Venus gravity field VGM2014 constructed by using the latest gravity and topography models, residual terrain model (RTM) and the Airy–Heiskanen isostatic compensation model. The VGM2014 is the first 10 km scale Venus gravity field model; the final results are representations of the 3-dimensional surface gravity accelerations and gravity disturbances for Venus. We found that the optimal global compensation depth of Venus is about 60 km, and the crustal density is potentially less than the commonly accepted value of 2700–2900 kg m^{-3}. This model will be potentially beneficial for the precise orbit determination and landing navigation of spacecraft around Venus, and may be utilized as a priori model for Venus gravity field simulation and inversion studies. The VGM2014 does not incorporate direct gravity information beyond degree 70 and it is not recommended for small-scale geophysical interpretation.

© 2014 Elsevier Inc. All rights reserved.

1. Introduction

Venus is the nearest terrestrial planet to the Earth and therefore is a significant target and important for space exploration efforts. A high resolution gravity field model can not only guarantee precise spacecraft navigation, but also provides global coverage rather than limited and local seismic, magnetic or other geophysical data. In addition, when combined with high resolution topographic data, knowledge of the gravity on Venus helps us to understand the interior structure of the planet.

Models of the venusian gravity field have been developed through the analyses of the spacecraft orbital tracking data. Venus gravity and topography models were initially generated by using tracking data from Venera 15/16 and Pioneer Venus Orbiter (PVO) spacecraft, these models were further improved by including the tracking data of Magellan spacecraft launched on March 4, 1989 that arrived at Venus on August 10, 1990. The most recent gravity field model for Venus is the MGNP180U (Konopliv et al., 1999) developed from Magellan orbital tracking data. The topography models produced include GTDR 3:2 (Rappaport et al., 1999)

and VenusTopo719. The spatial resolution of MGNP180U is around 100 km, while the topography model GTDR 3:2 generated from altimetry has the much higher resolution of about 5 km. As topography is recognized as one of the main contributors to the short-wavelength components in the gravity field of the Earth, Moon, and other terrestrial planets (Forsberg and Tscherning, 1981; Wieczorek, 2007), it can be used to improve and refine the gravity mapping of Venus with reasonable assumptions and modeling.

One useful approach is residual terrain model (RTM), constructed by subtracting a smooth surface from the topography. For example, Forsberg (1984) numerically integrated the topographic effect on the short-wavelength gravity, density anomaly and other geophysical parameters by dividing the terrain into rectangular prisms. Nagy et al. (2000) deduced the analytical expressions of gravitational potential and the first to second deviations of RTM. Hirt (2010), Hirt and Featherstone (2012) and Hirt et al. (2012) adopted this method to refine the short-wavelength gravity fields of the Earth, Moon and Mars successfully, and gave the hint that the models were possible to be used in spacecraft precise orbit determination and navigation.

All of the above applications did not take the isostatic compensation into account, which should not be overlooked for Venus even in short-wavelength (Kucinskas and Turcotte, 1994, 1996;
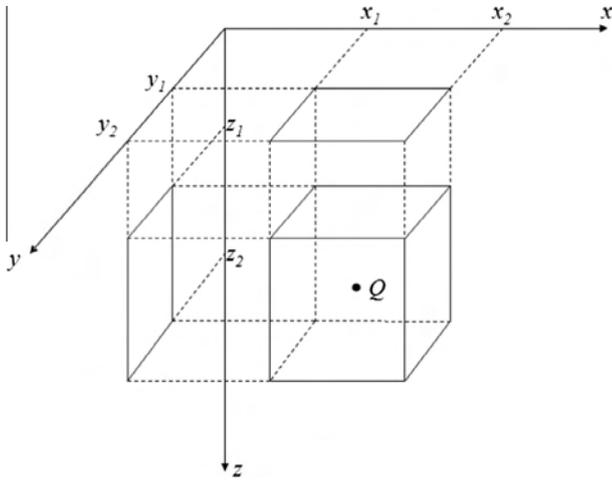
Fig. 1. The sketch map of rectangular prisms.

Grimm and Hess, 1997). Thus, in this paper, we refined the venusian gravity field model by RTM method and considered the global isostatic compensation correction. The current estimate of venusian crustal composition and density (2700–2900 kg m^{-3}) is deduced from rock samples of various landers (Grimm and Hess, 1997). Owing to the sparse sampling and specimens obtained from regolith rather than intact bedrock, the samples cannot reflect the actual composition of the venusian crust. At the same time, some regions, such as, Venera 13 and 14 landing sites have high porosity and materials as low as 1150–1500 kg/m^3 in density (Zolotov and Volkov, 1992). We adopt the average crust density of Venus with 2700 kg m^{-3} in our research.

We presented a refined venusian surface 3-dimensional gravity model VGM2014 (Venus Gravity Model 2013) with a resolution of 1/10°. The paper is arranged in the following order; the data and method is given in Section 2. In Section 3 data preprocessing is introduced. The results and analysis are presented in Section 4, and the conclusions are drawn in Section 5.

2. Data and methods

The latest venusian gravity model MGNP180U (Konopliv et al., 1999) is adopted in this paper. The spatial resolution of MGNP180U varies dramatically on the surface because of the spatial coverage of the orbital tracking data, with a resolution degree reaching up to 100 near the equator and a degree as low as 40 elsewhere on the planet (Konopliv et al., 1999; Wieczorek, 2007; James et al., 2013). The latest spherical harmonic model of the topography is the 719-degree VenusTopo719 from Wieczorek (http://www.ipgp.fr/~wieczor/SH/SH.html). This model is based on the sinusoidally projected GTDR 3.2 data set, with gaps filled by Pioneer Venus and Venera 15/16 data and interpolated using GMT software (Wessel and Smith, 1998). The topography models adopted in this paper are GTDR 3:2 and VenusTopo719.

VGM2014 is composed of three parts: (1) Venus surface normal gravity γ; (2) gravity disturbances of medium to long-wavelength using coefficients from degree 2 to degree 70 of the model MGNP180U, δg^{MGNP}; and (3) short-wavelength gravity disturbances obtained from RTM, δg^{VRTM} and isostatic compensation correction δg^{AH}.

To construct our model, we first introduced a reference rotating and homogeneous mass sphere with a mean venusian radius of R (6051.877 km, adopted from VenusTopo719) to deduce the normal gravity. The normal gravity on the surface is;

$$\gamma_0 = \frac{GM}{R^2} \tag{1}$$

where GM (3.24858592079 × 10^{14} m^3 s^{-2}, adopted from MGNP180U) is the product of the universal gravitational constant G and the venusian mass M.

Taking into account the venusian topography-dependent gravitational attraction, the normal gravity at the venusian surface is:

$$\gamma = \gamma_0 + H\frac{\partial\gamma}{\partial R} + \frac{H^2}{2}\frac{\partial^2\gamma}{\partial R^2} - z\cos(\varphi) \tag{2}$$

where H is height computed by subtracting the mean radius R from the planetocentric radius r. φ and λ are planetocentric latitude and longitude of the point, respectively. $z = \omega^2 R$ is the centrifugal acceleration at the equator. The venusian equatorial centrifugal acceleration is only 10^{-2} mgal order of magnitude as a result of extremely small angular speed of Venus's rotation (with the value of 2.9924 × 10^{-7} rad s^{-1}). Therefore, it was not necessary to take venusian centrifugal acceleration into account in the computation of our model.

The medium- and long-wavelength of gravity disturbance can be obtained from the gravity disturbance potential T. T can be directly represented by gravity spherical harmonic series expansions (Torge, 2001)

$$T(\varphi, \lambda, r) = \frac{GM}{r}\sum_{n=2}^{N}\left(\frac{R_0}{r}\right)^n\sum_{m=0}^{n}(\overline{C}_{nm}\cos m\lambda + \overline{S}_{nm}\sin m\lambda)\overline{P}_{nm}(\sin\varphi) \tag{3}$$

where N is the truncated degree, r, φ and λ are surface planetocentric radius, latitude, and longitude of the computation point, respectively. $R_0 = 6051$ km (from MGNP180U) is the reference radius. $\overline{C}_{nm}$ and $\overline{S}_{nm}$ are the fully-normalized spherical harmonic coefficients and $\overline{P}_{nm}$ is the fully-normalized associated Legendre functions of degree n and order m. Gravity disturbances δg^{MGNP} can be computed from the radial derivative of the disturbance potential:

$$\delta g^{MGNP}(\varphi, \lambda, r) = -\frac{\partial T}{\partial r}$$
$$= \frac{GM}{r^2}\sum_{n=2}^{N}(n+1)\left(\frac{R_0}{r}\right)^n\sum_{m=0}^{n}(\overline{C}_{nm}\cos m\lambda$$
$$+ \overline{S}_{nm}\sin m\lambda)\overline{P}_{nm}(\sin\varphi) \tag{4}$$

This part of gravity disturbance is computed from degree 2 to N from MGNP180U, which represents the medium- to long-wavelength of the gravity signal.

Gravity disturbances in the short-wavelength band can be refined through residual terrain model (RTM). The RTM serves as a spectral filter by subtracting a smooth reference surface from topography, thus contains voluminous high frequency gravity information. The short-wavelength gravity components of terrestrial planets are supported by the strength of the lithosphere rather than isostatic compensation (Torge, 2001; Watts, 2001; Mazarico et al., 2010).

To obtain accurate gravity information from RTM through numerical integration requires the knowledge of crust density point by point, currently an unachievable goal. However, considering that the venusian crust is predominantly composed of basalt, its average density is estimated to be between 2700 and 2900 kg/m^3 (Banerdt, 1986; Konopliv et al., 1999). As values in this range have an error less than 7.4%, we assume a constant density value of 2700 kg/m^3. We do not take the density variation into account given the lack of detailed topographic density distribution.

We computed the short-wavelength component of gravity disturbances δg^{VRTM} using the venusian RTM and the rectangular mass-prism (Forsberg and Tscherning, 1981; Nagy et al., 2000) with the key assumptions of a isostatically uncompensated topography and a constant crust density. The topographic residue $z^{RTM}(\varphi, \lambda)$ for each planetocentric point in venusian RTM was

computed by subtracting a harmonic reference surface from the real topographical radius $r(\varphi, \lambda)$

$$z^{RTM}(\varphi, \lambda) = r(\varphi, \lambda) - \sum_{n=0}^{N}\sum_{m=0}^{n}(\overline{HC}_{nm}\cos m\lambda + \overline{HS}_{nm}\sin m\lambda)\overline{P}_{nm}(\sin \varphi) \tag{5}$$

where the truncated degree N is consistent with the N in Eq. (3), $\overline{HC}_{nm}$ and $\overline{HS}_{nm}$ are the spherical harmonic coefficients of VenusTopo719.

The RTM can be represented by a grid of points, which can be regarded as prisms (Forsberg and Tscherning, 1981; Nagy et al., 2000) and are displaced as in Fig. 1. For each grid of point P, the gravitational potential of the terrain residue in the vicinity can be computed by numerical integration using Newton's law of universal gravitation. For each neighboring point Q, the height $z_Q^{RTM}(\varphi, \lambda)$ ranges from $z_1 = 0$ to $z_2 = z_Q^{RTM}(\varphi, \lambda)$, and the length and width ranging from x_1 to x_2, y_1 to y_2. The gravity disturbances raised by all of the prisms δg^{VRTM} are

$$\delta g^{VRTM} = hc - \sum_{1}^{k}G\rho\left|\left|\left|x\ln(y+c) + y\ln(x+c) - z\tan^{-1}\frac{xy}{zc}\right|_{x_1}^{x_2}\right|_{y_1}^{y_2}\right|_{z_1}^{z_2} \tag{6}$$

where ρ is the density of prism, c is the distance from point P and Q. The summation of the gravity effects is performed over k prisms within a radius around the computation point P, and the terrain residues beyond this radius are ignored. We took 400 km as the radius referring to the Moon and Mars cases (Hirt et al., 2012; Hirt and Featherstone, 2012). In addition, we tested it for Venus and verified that prisms outside this radius indeed have negligible gravitational effect on the computation point P. The values x_1, x_2, y_1, y_2 are computed from the planetocentric coordinates using a simple spherical projection.

$$x_1 = R\frac{2\pi}{360}\left(\lambda_Q - \lambda_P - \frac{\Delta\lambda}{2}\right)\cos\varphi_P, \quad x_2$$
$$= R\frac{2\pi}{360}\left(\lambda_Q - \lambda_P + \frac{\Delta\lambda}{2}\right)\cos\varphi_P$$

$$y_1 = R\frac{2\pi}{360}\left(\varphi_Q - \varphi_P - \frac{\Delta\lambda}{2}\right), \quad y_2 = R\frac{2\pi}{360}\left(\varphi_Q - \varphi_P + \frac{\Delta\lambda}{2}\right)$$

When the computation point P is located inside the residual topography, a correction term hc is required (Forsberg and Tscherning, 1981);
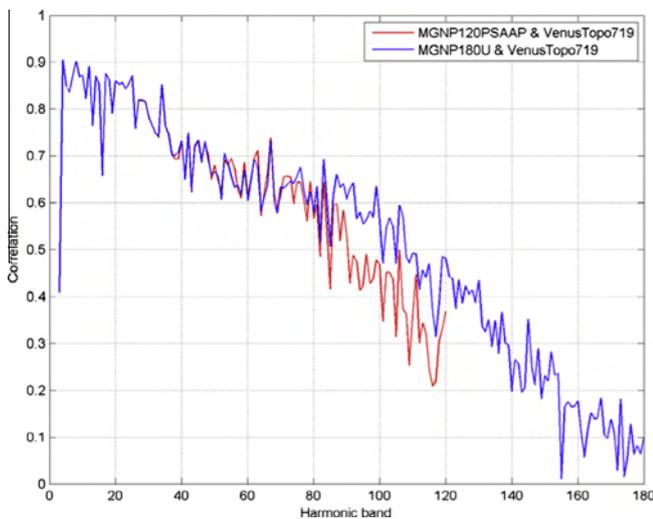

Fig. 2. The correlation between Venus gravity and topography.

$$hc = \begin{cases} 0, & z_P^{RTM} \geqslant 0 \\ 4\pi G\rho z_P^{RTM}, & z_P^{RTM} < 0 \end{cases} \tag{7}$$

The final factor to be considered in generating the gravity disturbance is the isostatic compensation correction. For the Earth, Moon, and Mars, topographic loads of 10–100 km dimensions are supported by the strength of the lithosphere rather than isostatic compensation, so it is reasonable to assume that the smaller scale of topographic features are also supported by the rigidity of the crust (Torge, 2001; Watts, 2001; Mazarico et al., 2010). However, Venus might be deeply and substantially isostatically compensated as asserted in studies of venusian gravity and topographic data (Kucinskas and Turcotte, 1994, 1996; Grimm and Hess, 1997). For this reason, isostatic correction is necessary even for short-wavelength topography.

In the current study, the ideal Pratt compensation is unlikely on Venus in view of the contradiction between the global compensation depth and the composition (James et al., 2013). For Airy compensation, the global compensation depth is generally recognized in the range of 30–50 km (Kucinskas and Turcotte, 1994, 1996; Grimm and Hess, 1997). Considering the range above, we assume Venus is in the state of global Airy compensation and choose the depth with 60 km through practical testing and contrast analysis (see Fig. 9(a)).

The compensation harmonic potential as calculated based on the Airy hypothesis is (Rummel et al., 1988)

$$\begin{Bmatrix}\overline{C}_{nm}^{Airy} \\ \overline{S}_{nm}^{Airy}\end{Bmatrix} = -\frac{3}{2n+1}\frac{\rho_c}{\bar{\rho}}\left[\left(\frac{R-D}{R}\right)^n\begin{Bmatrix}\overline{HC1}_{nm} \\ \overline{HS1}_{nm}\end{Bmatrix}\right.$$
$$-\frac{n+2}{2}\frac{\rho_c}{\rho_m - \rho_c}\left(\frac{R-D}{R}\right)^{n-3}\begin{Bmatrix}\overline{HC2}_{nm} \\ \overline{HS2}_{nm}\end{Bmatrix}$$
$$\left.+\frac{(n+2)(n+1)}{6}\left(\frac{\rho_c}{\rho_m - \rho_c}\right)^2\left(\frac{R-D}{R}\right)^{n-6}\begin{Bmatrix}\overline{HC3}_{nm} \\ \overline{HS3}_{nm}\end{Bmatrix}\right] \tag{8}$$

where ρ_c is the average crust density, ρ_m = 3200 kg/m³ is the average mantle density (Banerdt, 1986), $\bar{\rho}$ is venusian global average density, D is the global compensation depth, $\overline{HC1}_{nm}, \overline{HS1}_{nm}, \overline{HC2}_{nm}, \overline{HS2}_{nm}, \overline{HC3}_{nm}, \overline{HS3}_{nm}$ are the fully-normalized spherical harmonic coefficients from

$$\begin{Bmatrix}\overline{HC1}_{nm} \\ \overline{HS1}_{nm}\end{Bmatrix} = \frac{1}{4\pi}\int_{\sigma}\frac{r(\varphi, \lambda) - R}{R}\begin{Bmatrix}\cos m\lambda \\ \sin m\lambda\end{Bmatrix}\overline{P}(\sin\varphi)d\sigma$$

$$\begin{Bmatrix}\overline{HC2}_{nm} \\ \overline{HS2}_{nm}\end{Bmatrix} = \frac{1}{4\pi}\int_{\sigma}\left(\frac{r(\varphi, \lambda) - R}{R}\right)^2\begin{Bmatrix}\cos m\lambda \\ \sin m\lambda\end{Bmatrix}\overline{P}(\sin\varphi)d\sigma \tag{9}$$

$$\begin{Bmatrix}\overline{HC3}_{nm} \\ \overline{HS3}_{nm}\end{Bmatrix} = \frac{1}{4\pi}\int_{\sigma}\left(\frac{r(\varphi, \lambda) - R}{R}\right)^3\begin{Bmatrix}\cos m\lambda \\ \sin m\lambda\end{Bmatrix}\overline{P}(\sin\varphi)d\sigma$$

Therefore, the isostatic correction δg^{Airy} corresponding to terrain residual gravity disturbances δg^{VRTM} are

$$\delta g^{AH} = \frac{GM}{r^2}\sum_{n=N+1}^{n_{max}}(n+1)\left(\frac{R_0}{r}\right)^n\sum_{m=0}^{n}\left(\overline{C}_{nm}^{Airy}\cos m\lambda + \overline{S}_{nm}^{Airy}\sin m\lambda\right)\overline{P}_{nm}(\sin\varphi) \tag{10}$$

where n_{max} is consistent with the gravity resolution.

In summary, the ultimate output is 3-dimensional venusian surface gravity accelerations g^{VGM} and gravity disturbances δg^{VGM}

$$\delta g^{VGM} = \delta g^{MGNP} + \delta g^{VRTM} + \delta g^{AH} \tag{11}$$
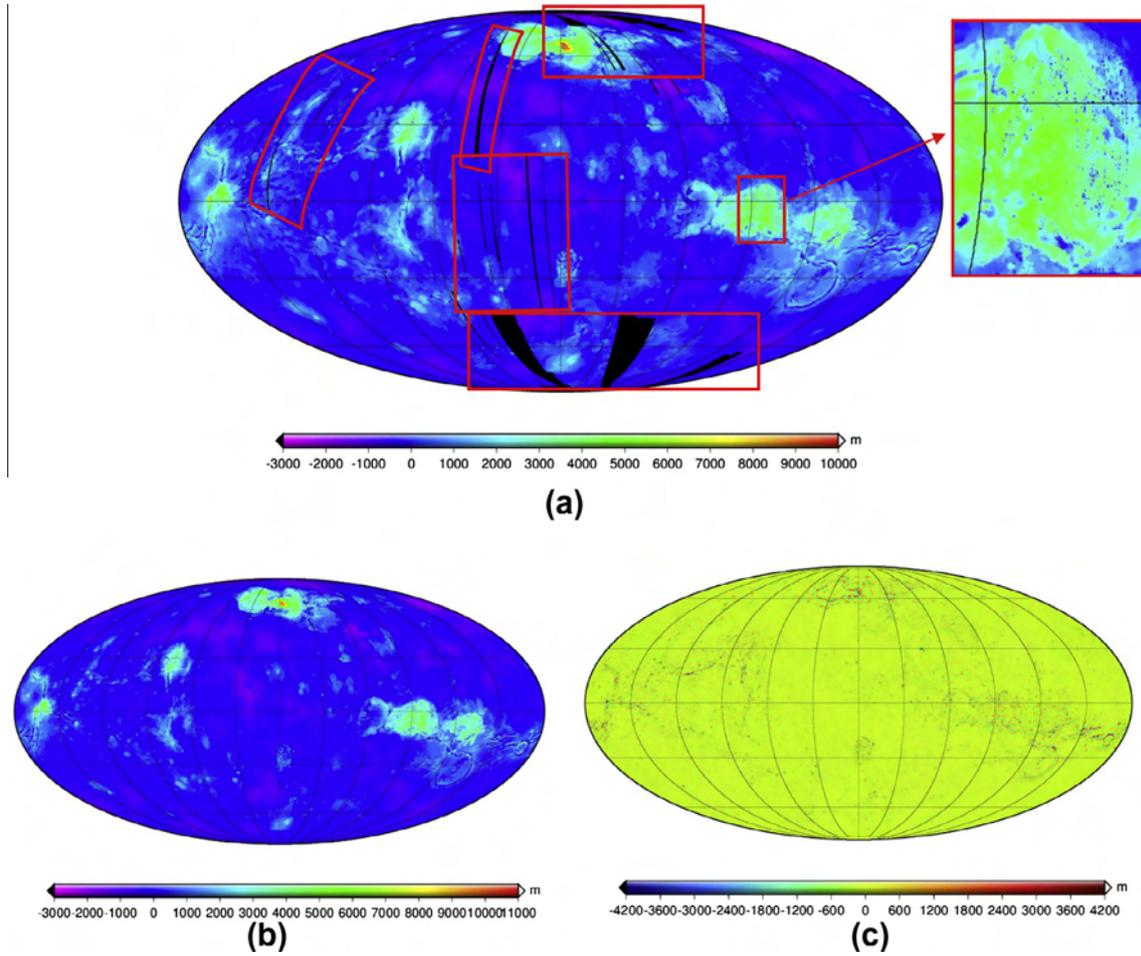
$$g^{VGM} = \gamma + \delta g^{VGM} \tag{12}$$

Fig. 3. Topographic data: (a) topography map of GTDR 3:2 referenced to a radius of 6051877 m. (b) Topography in this paper referenced to a radius of 6051877 m. (c) Residual terrain map (RTM) of Venus. Mollweide projection with a central meridian of 0° longitude. Meridians and parallels are 30° apart.

3. Data preprocessing

In order to refine the short-wavelength gravity by topography, we need a fitting truncated degree N for gravity and topography models to separate the short-wavelength component from the medium- and long-wavelength of the gravity signal. Correlation between gravity and topography is used here as a criteria. It is obtained from gravity and topography spherical harmonic coefficients (Wieczorek, 2007):

$$\gamma(l) = \frac{S_{fg}(l)}{\sqrt{S_{ff}(l)S_{gg}(l)}} \tag{13}$$

where $S_{gg}(l)$ and $S_{ff}(l)$ are power spectrum of gravity and topography, respectively.

$$S_{gg}(l) = \sum_{m=2}^{l}(\bar{S}_{lm}^2 + \bar{C}_{lm}^2), \quad S_{ff}(l) = \sum_{m=2}^{l}(\overline{HS}_{lm}^2 + \overline{HC}_{lm}^2) \tag{14}$$

$S_{fg}(l)$ is the cross-power of gravity and gravity

$$S_{fg}(l) = \sum_{m=2}^{l}\left(\bar{S}_{lm}\overline{HS}_{lm} + \bar{C}_{lm}\overline{HC}_{lm}\right) \tag{15}$$

The correlation spectra between the gravity and topography are plotted in Fig. 2. It is below 0.7 and decreases drastically beyond degree 70, which indicates that the attenuating gravity signal

beyond degree 70 is caused by an inaccurate shot-wavelength component in the gravity field model. Therefore, we took 70 as the truncated degree.

The other important issue in data preprocessing is the topography data. The sinusoidally projected GTDR 3:2 data set was adopted here. The model has a resolution of 0.0439° and is displayed in Fig. 3(a). It is clear that GTDR 3:2 has many long and narrow areas of uncovered image gaps, accompanied with dotted orbiter error in red[1] boxes. We filled the gaps with grid data converted from VenusTopo719 and smoothed the data to reduce the dotted error. In the end, we derived a topography model at a resolution of 0.1° through a quadratic interpolation taking account of the original data resolution and quality.

4. Results and analyses

The gravity disturbances of the medium-, long-wavelength, and the short-wavelength as discussed in Section 2 are shown in Fig. 4(a and b), respectively. The 3-dimensional Venus surface gravity disturbances, which are the sum of the three parts, are shown in Fig. 4(c). By combining these parts with the surface normal gravity as described in Section 2, 3-dimensional venusian surface gravity accelerations were estimated. These results are visualized in Fig. 4(d).

---

[1] For interpretation of color in Fig. 3, the reader is referred to the web version of this article.
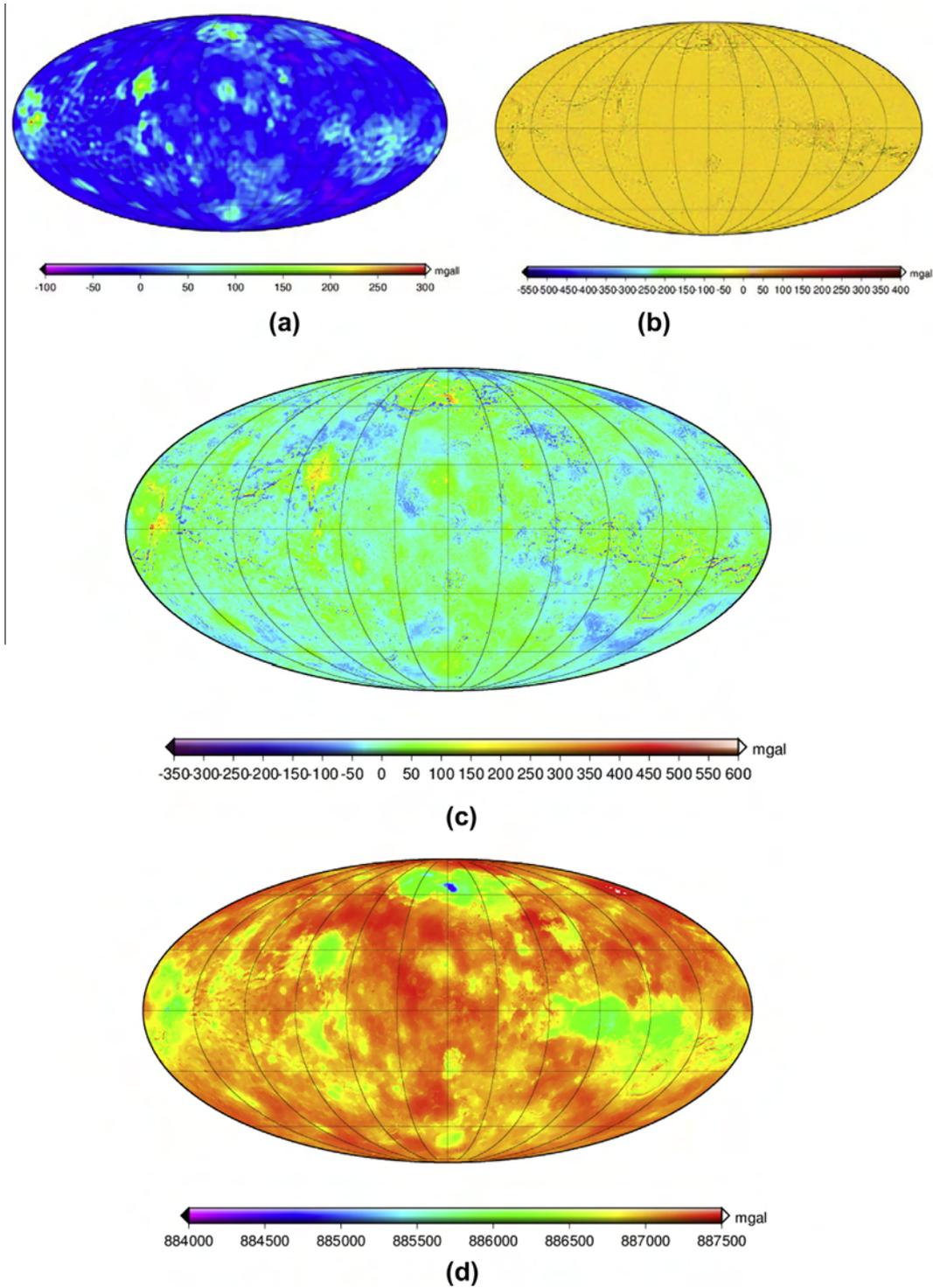
Fig. 4. VGM2014 output: (a) gravity disturbances of medium- and long-wavelength. (b) Gravity disturbances of short-wavelength. (c) VGM20013 surface gravity disturbances. (d) VGM20013 surface gravity acceleration. Mollweide projection with a central meridian of 0° longitude. Meridians and parallels are 30° apart.

Figs. 5 and 6 show the gravity disturbances of the regions of Beta Regio (10–40°N, 65–90°W) and Atla Regio (20°S–25°N, 155–180°W); famous for their volcanic feature similar to the Earth, in order to show the effects of different wavelength components on the final gravity disturbances more clearly. The Beta Regio is one of the earliest landform recognized in northern mid-latitudes of Venus. The main topographic feature is the Beta Highland (a lithosphere uplift driven by a hot plume) cut by the Devana Chasma (a deep tectonic valley from south to north) (Basilevsky

and Head, 2007). The Atla Regio lies along the equator, and is composed of numerous overlapping lava flows. The main geomorphological features there are three large volcanoes, including Ozza Mons in the south-east, the Maat Mons in the south-west, and the Sapas Mons in the north-west, as well as three rifts, including Ganis Chasma, Dali Chasma and Parga Chasma that form a triple junction at the base of Ozza Mons (Senske and Head, 1992). The gravity from medium- and long-wavelengths reflects the uplift, volcanoes, and other large-scale gravity, while the gravity from
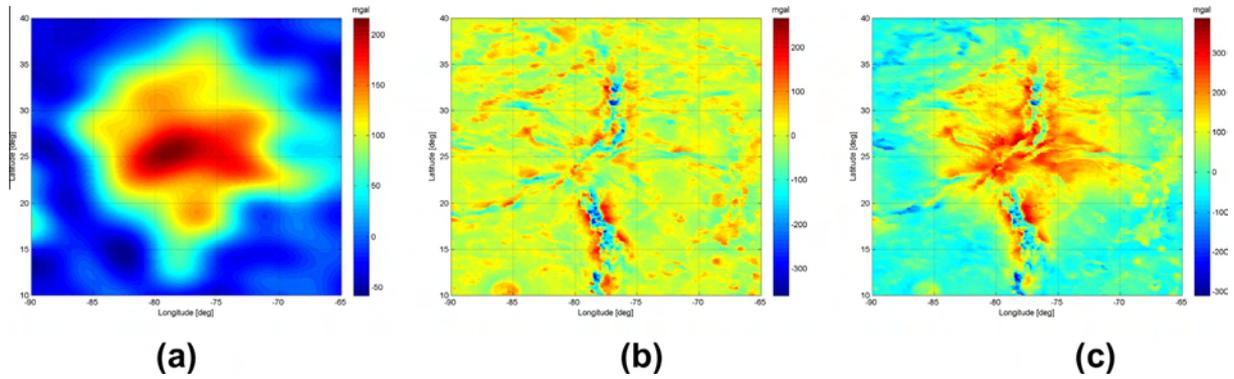
Fig. 5. Gravity disturbances of different wavelengths at Beta Regio (in mgal): (a) middle- and long-wavelength part. (b) Short-wavelength part. (c) Summation of (a and b).
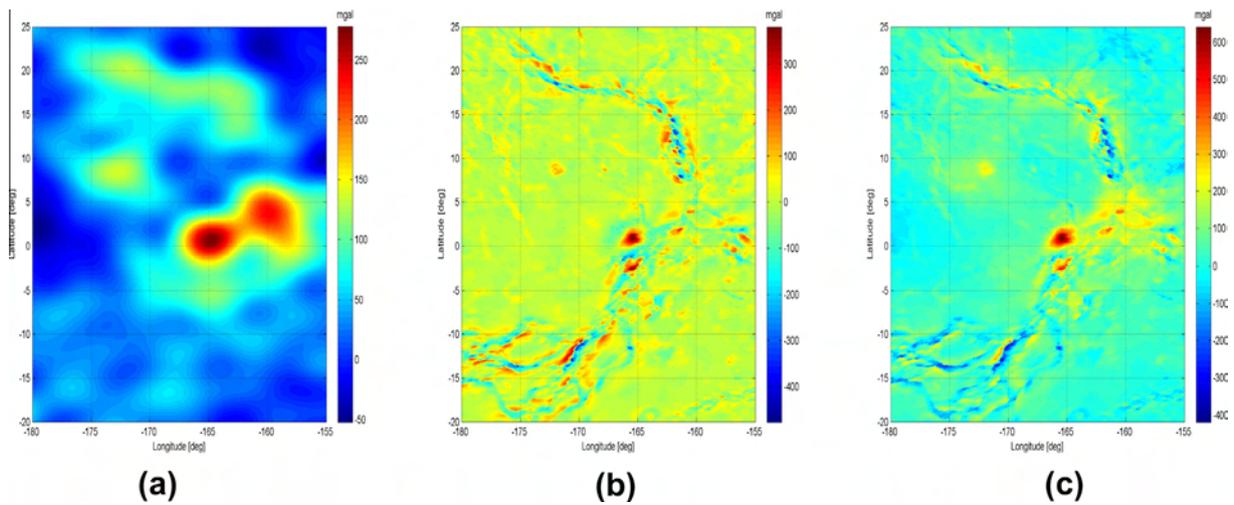

Fig. 6. Gravity disturbances of different wavelength at Atla Regio (in mgal): (a) middle- and long-wavelength part. (b) Short-wavelength part. (c) Summation of (a and b).

Table 1
Basic statistical information of VGM2014 model (in mgal).

Parameters	Max	Min	Average	STD
VGM2014 surface gravity acceleration	887610.8	884291.9	887006.7	2353.9
VGM2014 surface gravity disturbances	641.8	−506.5	−3.4	378.3
MGNP180U (band 2–70) surface gravity disturbances	277.7	−83.6	−3.5	373.9
VRTM70+AH60[a] surface gravity disturbances	380.7	−590.5	0.1	53.9

[a] AH60 indicates the depth of Airy–Heiskanen global isostatic compensation with 60 km. It is also shown in Fig. 9(a).

Table 2
Gravity disturbance peaks at the surface of venusian features of interest for three gravity models (in mgal).

| Regions	Longitude range	Latitude range	MGNP120PSAAP	MGNP180U	VGM2014
Maxwell	50°W to 20°E	55–80°N	236.1	254.0	430.1
Phoebe	80–65°W	10°N to 25°S	123.2	163.7	310.6
Akna	40–50°W	65–70°N	116.4	144.8	324.0
Freya	19–24°W	75–71°N	124.1	144.8	270.6
Bell	44–52°E	27–33°N	162.2	212.1	420.5
Beta	65–90°W	10–40°N	234.3	286.7	388.3
Atla	155–180°W	25°N to 20°S	379.3	486.3	641.8
Gula	0–5°W	20–24°N	134.0	136.1	310.4
Maat	163–168°W	2°N to 1°S	379.3	486.3	641.8
Ozza	158–162°W	2–5°N	224.6	260.8	400.0
Nokomis	165–175°W	15–25°N	145.9	168.4	327.5
Sapas	170–175°W	8–10°N	170.3	202.9	279.3
Atalanta	150–175°E	55–75°N	−85.0	−86.2	−124.1
Mead	56–60°E	10–15°N	−67.4	−105.1	−94.3
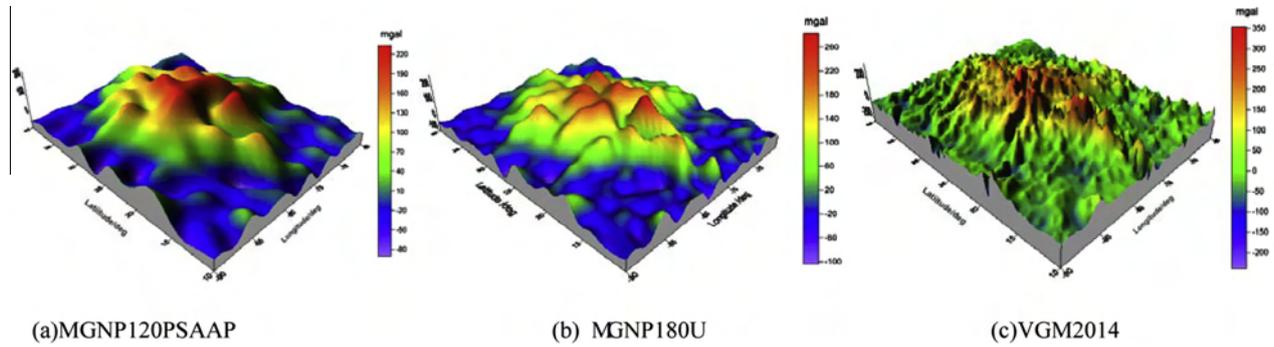
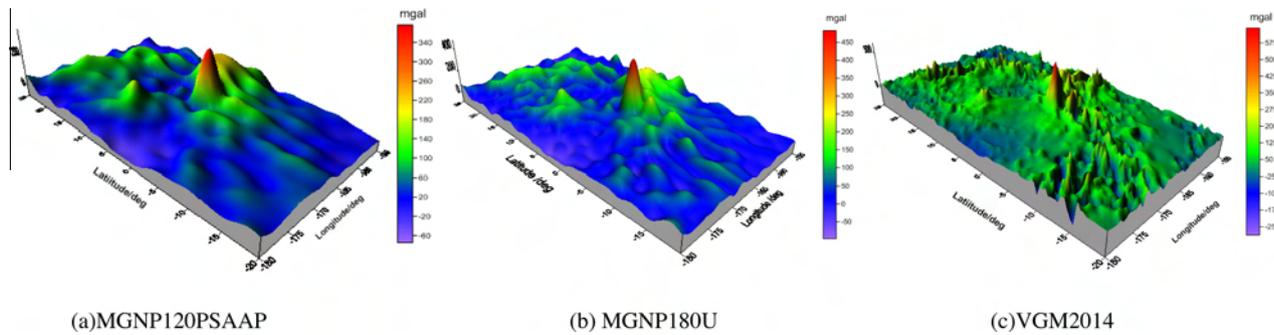**Fig. 7.** Gravity disturbances at Beta Regio (in mgal).

Fig. 8. Gravity disturbances at Atla Regio (in mgal).

short-wavelength reflects smaller-scale gravity effects from rifts and ridges.

In general, venusian surface gravity disturbances are small, a consequence of the smooth topography, with some exceptions in certain regions with more complex geomorphology. The gravity disturbances in the MGNP180U model are within the range of −200 to 500 mgal, while the ones in the proposed VGM2014 model have a larger range of −500 to 600 mgal as a result of short-wavelength topographical refinements. Short-wavelength refinement to the gravity field model has a significant effect on highland and lowland areas as illustrated in Fig. 4(c). From Table 1, the minimum gravity acceleration estimated in the proposed VGM2014 model is located in the Maxwell Regio and with a value of 8.842919 m s^{-2}. The minimum value of the MGNP180U (8.840035 m s^{-2}) is different but with same location.

In Table 2 we can see that the proposed VGM2014 model has a substantial effect on the amplitudes of almost all the major gravitational features on Venus as compared with the MGNP120PSAAP and MGNP180U models. The MGNP120PSAAP and MGNP180U are models with a degree and order of 120 and 180, respectively, and were developed using different amount of orbiter tracking data from various spacecraft (Konopliv et al., 1996, 1999). Table 2 reveals that in different models the Sapas, Mead, and Atalanta plains display minor differences, depending on how limited short-wavelength structures are treated. The peak is situated on Maat Mons of the Atla Regio regions, which is the same in all three models.

The gravity disturbances of the MGNP180U and proposed VGM2014 models of the Beta Regio and Atla Regio are illustrated in Figs. 7 and 8, respectively. The proposed VGM2014 model is consistent with the MGNP180U model at a large scale, but show much more detail at a smaller scale such as small rifts and ridges.

A direct check is not possible as there are no ground-truth observations, and we try to assess the model VGM2014 in spectrum domain. A similar method to generate high resolution

gravity field using topography data has been successfully applied to the Earth, Moon, and Mars (Hirt, 2010; Hirt et al., 2012; Hirt and Featherstone, 2012), and indirectly testified the feasibility of the RTM. Thus, in order to analyze the spectral character of the proposed VGM2014 model, we converted the 3-dimensional grid data to a reference surface at the highest radius of the topography and then transformed the 1/10° 2-dimensional grid to 899-degree spherical harmonic coefficients with SHTOOLS software. Fig. 9(a) compares the RMS spectra power of MGNP180U and VGM2014. The RMS spectra power of MGNP180U decreases significantly beyond degree 70, whereas the VGM2014 retains intensive power, indicating that VGM2014 greatly improved the high-degree part of venusian gravity field.

Fig. 9(a) also shows a comparison of the RMS spectra power of the proposed VGM2014 model with different isostatic compensation depths of 30 km, 40 km, 50 km, and 60 km respectively. In contrast to the jump around degree 70 of depth with uncompensated, 30 km, 40 km, and 50 km, the RMS spectra power with a depth of 60 km is smooth at degree 70 without distinct vibrations in the proposed VGM2014 model. It indicates that the 60 km depth of compensation is more reasonable. In addition, although isostatic correction makes a difference on the scale range with degrees from 71 to 400, it has little effect at the smaller scale (with degrees higher than 400). It may suggest that for small scale topography (degree higher than 400) it is supported by the rigidity of Venus crust.

It is obvious in Fig. 9(a) that the power in high degrees (beyond degree 200) is much stronger than the Kaula curve. Considering all of the procedures to build our VGM2014 model, there are two assumptions that can influence the final results: the average crustal density and the global isostatic compensation depth. According to the analysis above, the isostatic compensation depth has minor influence on the high frequency (especially with degrees higher than 400), then the reason for the much stronger power in high degrees would only come from the assumption of the average crustal density. Therefore, we suggest the deviation between the
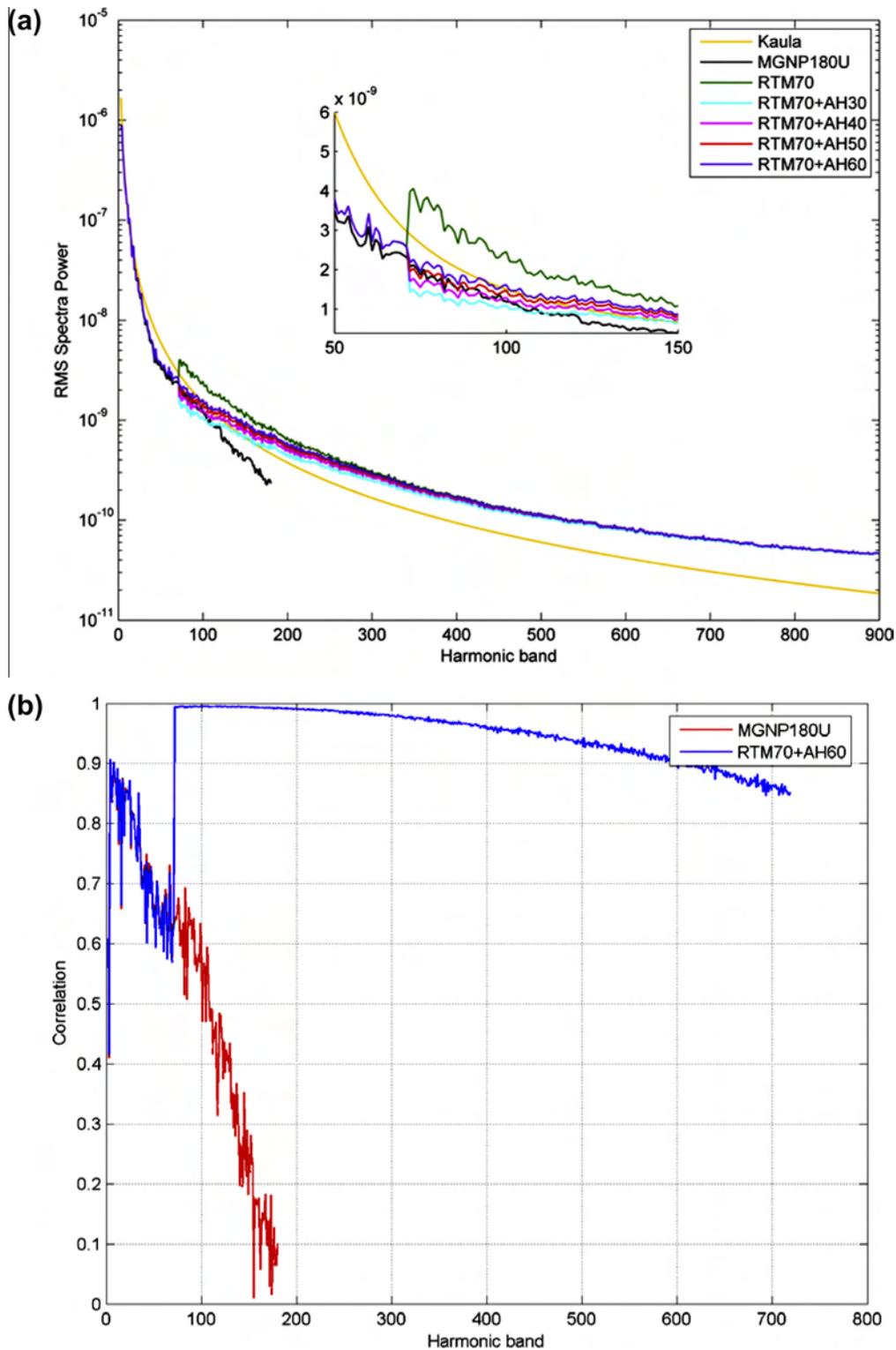
Fig. 9. (a) Gravity RMS spectra power of MGNP180U and VGM2014 with isostatic compensation depth of 30 km, 40 km, 50 km and 60 km. Kaula constraint coefficient is 1.5×10^{-5}. (b) Correlation of topography (VenusTopo719) and gravity (MGNP180U and VGM2014) with isostatic compensation depth 60 km.

VGM2014 and Kaula constraint may indicate that the average crustal density value adopted in this paper (2700 kg m^{-3}) is bigger than actual average Venus crustal density.

Fig. 9(b) shows the correlation of topography (VenusTopo719) and gravity (MGNP180U and VGM2014) with isostatic compensation depth of 60 km. In contrast to MGNP180U, the proposed VGM2014 has a much higher correlation of topography and gravity

after degree 70. It implies that the VGM2014 model truly makes good use of the short-wavelength topographic information.

5. Conclusion

In this paper, we proposed a new 3-dimensional Venus gravity field model VGM2014. The proposed VGM2014 model is the first

10 km resolution venusian gravity field. The VGM2014 model was constructed with the assumptions of a constant crustal density and global Airy isostatic compensation. Compared with the current Venus gravity field model MGNP180U, the VGM2014 model can reveal high resolution gravity information, especially for mountain regions, such as the Beta Regio and Atla Region. By using the spectrum analysis of the VGM2014 model, we found that the optimal global compensation depth of Venus is about 60 km, and the crustal density may be less than 2700–2900 kg m^{-3}. The VGM2014 is potentially beneficial for orbit determination and landing navigation, and can be used as a priori model for Venus gravity field simulations and inversion studies. We cannot provide uncertainty information for the proposed VGM2014 such as when the gravity field is solved from the dynamic orbit determination method (Konopliv et al., 1999). In our method it is difficult to build linear relationship between gravity field coefficients and topography data to make use of the error propagation law (Lawson and Hanson, 1995). Given that the proposed VGM2014 model does not incorporate gravity field observations beyond degree 70, it is not recommended for direct geological and smaller-scale geophysical interpretation.

Acknowledgments

Appendix A. Supplementary material

Supplementary data associated with this article can be found, in the online version, at http://dx.doi.org/10.1016/j.icarus.2014.09.052.

References

Banerdt, W.B., 1986. Support of long-wavelength loads on Venus and implications for internal structure. J. Geophys. Res. 91 (B1), 403–419.

Basilevsky, A.T., Head, J.W., 2007. Beta Regio, Venus: Evidence for uplift, rifting, and volcanism due to a mantle plume. Icarus 192, 167–186.

Forsberg, R., 1984. A Study of Terrain Reductions, Density Anomalies and Geophysical Inversion Methods in Gravity Field Modelling (No. OSU/DGSS-355). Geod. Sci. Ohio State Univ., Columbus.

Forsberg, R., Tscherning, C.C., 1981. The use of height data in gravity field approximation by collocation. J. Geophys. Res. 86 (B9), 7843–7854.

Grimm, R.E., Hess, P.C., 1997. The crust of Venus. In: Venus II. Univ. of Arizona Press, Tucson.

Hirt, C., 2010. Prediction of vertical deflections from high-degree spherical harmonic synthesis and residual terrain model data. J. Geodesy 84, 179–190.

Hirt, C., Featherstone, W.E., 2012. A 1.5 km-resolution gravity field model of the Moon. Earth Planet. Sci. Lett. 329–330, 22–30.

Hirt, C., Claessens, S.J., Kuhn, M., et al., 2012. Kilometer-resolution gravity field of Mars: MGM2011. Planet. Space Sci. 67, 147–154.

James, P.B., Zuber, M.T., Phillips, R.J., 2013. Crustal thickness and support of topography on Venus. J. Geophys. Res. Planets 118, 859–875.

Konopliv, A.S., Sjogren, W.L., Yoder, C.F., et al., 1996. Venus 120th degree and order gravity field. American Geophysical Union (Fall). San Francisco, CA.

Konopliv, A.S., Banerdt, W.B., Sjogren, W.L., 1999. Venus gravity: 180th degree and order model. Icarus 139, 3–18.

Kucinskas, A.B., Turcotte, D.L., 1994. Isostatic compensation of equatorial highlands on Venus. Icarus 112, 104–116.

Kucinskas, A.B., Turcotte, D.L., 1996. Isostatic compensation of Ishtar Terra, Venus. J. Geophys. Res. 101, 4725–4736.

Lawson, C.L., Hanson, R.J., 1995. Solving Least Squares Problems. SIAM Classics in Applied Mathematics, vol. 15. Society for Industrial and Applied Mathematics, Philadelphia.

Mazarico, E., Lemoine, F.G., Han, S.C., et al., 2010. GLGM-3: A degree-150 lunar gravity model from the historical tracking data of NASA Moon orbiters. J. Geophys. Res. 115 (E0500), 1.

Nagy, D., Papp, G., Benedek, J., 2000. The gravitational potential and its derivatives for the prism. J. Geodesy 74, 552–560.

Rappaport, N.J., Konopliv, A.S., Kucinskas, A.B., 1999. An improved 360 degree and order model of Venus topography. Icarus 139, 19–31.

Rummel, R., Rapp, R.H., Sunkel, H., et al., 1988. Comparisons of Global Topographic Isostatic Models to the Earth's Observed Gravity Field. Geod. Sci., Ohio State Univ., Columbus.

Senske, D.A., Head, J.W., 1992. Atla Regio, Venus: Geology and origin of a major equatorial volcanic rise. Lunar Planet. Sci. 789, 107–109.

Torge, W., 2001. Geodesy, third ed. de Gruyter, Berlin.

Watts, A.B., 2001. Isostasy and Flexure of the Lithosphere. Cambridge University Press.

Wessel, P., Smith, W.H.F., 1998. New, improved version of the Generic Mapping Tools released. EOS: Trans. Am. Geol. Union.

Wieczorek, M.A., 2007. Gravity and topography of the terrestrial planets. Treatise Geophys. 10, 165–206.

Zolotov, M.Y., Volkov, V.P., 1992. Chemical processes on the planetary surface. In: Venus Geology, Geochemistry and Geophysics: Research Results from the Soviet Union. Tucson Univ. of Arizona Press.